JOURNAL OF GUIDANCE, CONTROL, AND DYNAMICS
Vol. 23, No. 3, May–June 2000

Adaptive Hysteresis Model for Model Reference Control with Actuator Hysteresis

G. Webb*
Texas A&M University, College Station, Texas 77843
A. Kurdila†
University of Florida, Gainesville, Florida 32611
and
D. Lagoudas‡
Texas A&M University, College Station, Texas 77843

When working with active materials which exhibit profound hysteresis, such as shape memory alloys, the "perfect" mathematical representation of the hysteresis does not exist. However, we can represent many hysteretic trends by means of operator models that vary in their theoretical, physical, and computational complexity, depending on how precisely they model the hysteresis. In previous studies by the authors, generalized Preisach representations of the hysteresis phenomena by use of Krasnosel'skii and Pokrovskii (KP) operators have been represented in linear parametric form. This parameterized KP model has been successfully implemented with a gradient-adaptive law for on-line identification and adaptive compensation when the hysteresis output can be measured. The applicability of the parameterized KP model is extended to model reference control systems with hysteresis actuators whose output cannot be measured.

I. Introduction

ALTHOUGH there has been unprecedented interest in utilizing the class of so-called active materials for control actuation in diverse engineering applications, numerous fundamental modeling issues remain open when these actuators are used in realistic cases. Perhaps one of the most significant challenges remaining for those interested in developing refined models for active material actuators is the derivation of accurate, low-dimensional representations of hysteresis inherent in these devices. For example, although it is accepted that linear models provide reasonable representations of piezoceramic actuators operated at low electric-field strengths, this class of devices is routinely operated at high field strengths and exhibits nonnegligible hysteretic effects.[1,2] Similarly, shape memory alloy (SMA) actuating materials exhibit profound hysteresis in their thermomechanical response.[3,4] Similar observations have been made for the recently introduced class of magnetorheological fluids.[5]

When a control law is designed for systems with hysteretic actuators, it is desirable to know the degree to which the hysteresis nonlinearity may be linearized. The control signal u_d, generated by a given control scheme, is normally proportional to the output value of the actuator u, whereas the actual input variable to the coupled actuator/plant system is the quantity v, the input to the actuator. An effective method for linearizing the hysteresis involves compensation that relies on the identification of the hysteresis model $H(v)$ to create an inverse model such that $v = H^{-1}(u_d)$. There are operator-theoretical models that can reasonably predict static, scalar hysteresis for actuators such as SMA, piezoceramics, and electro/magnetorheological fluids. These models, identified off line from experimental data, are effective in open-loop compensation only when they match well the exact hysteresis. However, when there are significant differences between the identified model and the exact hysteresis, open-loop compensation can inject artificial input disturbances into the system: $u(t) = u_d(t) + e_H(t)$.

General theories for the mathematical representation of hysteresis operators are relatively new. The seminal work of Krasnosel'skii and Pokrovskii[6] (KP) has only recently been translated into the English language. Significant recent contributions to the general theory of hysteresis operators also includes the works by Visintin[7] and Mayergoyz.[8] Given the widespread interest in actuation devices in which active materials in general are used, it is inevitable that some research that treats hysteresis in control has appeared in the literature and research. For example, Ge and Jouaneh[2] use the formulation of Mayergoyz[8] to implement a simple proportional, integral, and differential control scheme that considers hysteresis in piezoceramic actuation. Hughes and Wen[1] derive linearizing compensators for both piezoceramic and SMA actuators. Other significant efforts for modeling hysteresis operators as they appear in classes of partial differential equations are described by Verdi and Visintin.[9,10]

A recently introduced method for control of hysteretic actuators involves an adaptive-hysteresis model for on-line identification and closed-loop compensation.[11] The hysteresis model is an extension of the Preisach model that uses KP's generalized play operator to form the basic hysteresis operators. This model is denoted as the KP-hysteresis model, which can be represented in linear parametric form[11,12] suitable for gradient-adaptive control.[13] In this methodology, it is assumed that a control law exists for the system that commands an output signal from the actuator. The KP model (forward and inverse) is adapted to match the actual hysteresis, with the updated inverse KP model mapping the control signal into an actuator input signal. Numerical results for a general hysteretic actuator and experimental results with SMA actuators have shown the robust performance of the adaptive KP model for closed-loop control and on-line identification.[11,12] In addition, the adaptive update of the hysteresis model for SMA actuators allows for real-time prediction of quantities such as actuator saturation and width of hysteresis.

The gradient-adaptive KP model[11] depends on measurements (actual or estimated) of the hysteresis output. Because the gradient-adaptive law depends on knowing only the input and the output of the actuator, adaptive compensation can be carried out independently of any knowledge of the actuated system. However, there may be instances when it is difficult to measure, or even estimate, the hysteresis output and one must rely on only system output measurements. The work in this paper is motivated by Tao and Kokotovic[14,15] (TK), who proposed an adaptive-inverse approach for adaptive control of systems with hysteresis when the hysteresis output cannot be measured. They stated that "a general hysteresis

Received 6 August 1997; revision received 5 April 1999; accepted for publication 28 April 1999.

*Research Associate, Department of Aerospace Engineering. Member AIAA.
†Professor, Department of Aerospace Engineering, Mechanics and Engineering Science. Member AIAA.
‡Professor, Department of Aerospace Engineering. Member AIAA.

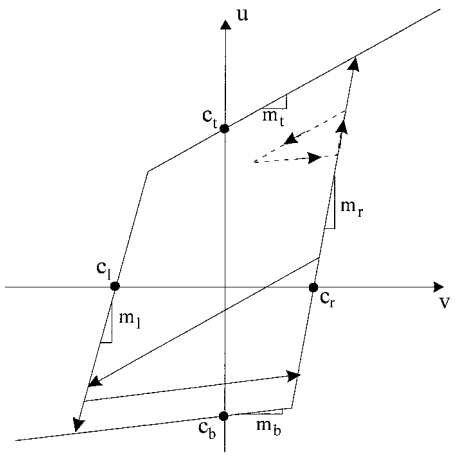

Fig. 1 Representation of TK's [14] hysteresis model.

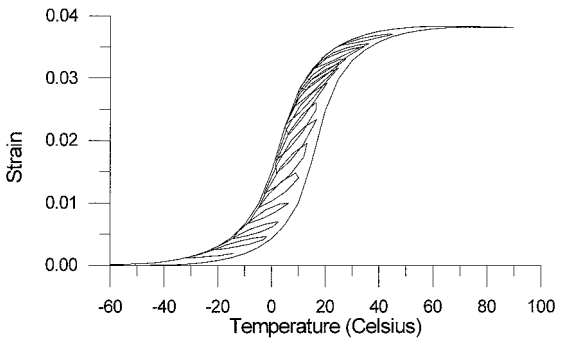

Fig. 2 Typical hysteresis exhibited by SMA.

model would not be convenient because of its complexity"[14] and designed a simplified hysteresis model useful for parameter adaptive control. Figure 1 shows TK's simplified model, parameterized by the constants m_t, c_t, m_b, c_b, m_r, c_r, m_l, and c_l that determine two half lines and two line segments that bound the hysteresis. In reality, even the best identification of hysteresis will result in a nonzero hysteresis modeling error, which is a function of the parameter error and the error that is due to characteristics that are not represented by the hysteresis model. By comparing Fig. 1 with the hysteresis typically exhibited by SMA, shown in Fig. 2, one can see that the TK model fails to represent many of the hysteresis characteristics. Therefore, even if an optimal time-averaged set of parameters is learned for the TK model through adaptation, the error that is due to unmodeled hysteresis characteristics will remain large.

It stands to reason that, given two hysteresis models, the one that more accurately represents the physical hysteresis characteristics will also provide for the smaller hysteresis modeling error. Although the TK model is physically simplistic, it is numerically complicated. This paper presents the framework for implementing the more physically accurate, parameterized KP model in adaptive-inverse compensation for systems for which the hysteresis output cannot be measured. The parameterized KP-hysteresis model is described in Sec. II. Section III provides some background for model reference control (MRC) and the accompanying theory for fixed- and adaptive-hysteresis compensation in MRC. The necessary theorems for the stability of adaptive-inverse compensation that use the parameterized KP model in MRC are given. The results of several numerical examples are given in Sec. IV, in which the hysteresis plant is numerically represented by a model that closely resembles the physical hysteresis characteristics exhibited by active materials.

II. Hysteresis Model

The parameterized KP model, developed in Refs. 11 and 16, represents the hysteretic dependence of the actuator output on the input. The KP model is founded on the principle first introduced by Preisach,[8,17] in which the output is an infinite sum of weighted simple hysteresis operators, or kernels. Krasnosel'skii and Pokrovskii[6] developed a continuous version of the Preisach kernel, which allowed for finite-dimensional approximations of the infinite-dimensional model. Banks et al.[16,18] studied the mathematical properties of the infinite-dimensional KP model and proved the well posedness for the inverse problem of off-line identification of a finite-dimensional approximation. Webb[11] studied the finite-dimensional, parameterized version of the KP model for adaptive identification and compensation for control of hysteretic actuators. Webb et al.[12] provided experimental results for control of an SMA wire actuator by using the adaptive KP model along with an adaptive thermal model to control the current input to the wire. Although only a summary of the parameterized KP model is given in this paper, the interested reader is directed to the above references for an in-depth background.

The parameterized KP model for use in adaptive control is developed to solve the following problem: Given a hysteretic input–output relationship, define a model that

1) is linear in the parameters $\boldsymbol{\theta} = \{\theta_i\}^T$, $i = 1, \ldots, N$ and
2) can be represented in vector form:

$$[H(v)](t) = \boldsymbol{\theta}^T [\boldsymbol{F}(v)](t), \qquad [\boldsymbol{F}(v)](t) = [\{f_i(v)\}^T](t) \qquad i = 1, \ldots, N \quad (1)$$

where $[f_i(v)](t)$ are independent functions of the input.

The notation $[\cdot](t)$ represents the fact that the operator in $[\cdot]$ is dependent on the trajectory, $v \in C^0[0, t]$, not an instantaneous value $v(t)$.

For the model to represent the hysteresis, the functions of input must have the capability of accounting for the previous input history in determining the output. The Preisach model concept—a summation of weighted hysteresis operators—provides the structure for such a model. However, the mathematical properties of the Preisach model are well defined for only an infinite summation of Preisach operators.[16,18] For practical applications, we require a model that is well defined in finite dimensions, for which a class of operators known as KP operators has been shown to be well suited.[16] The actions of the Preisach and the KP operators are shown in Fig. 3. The Preisach operator can exist at only two states, $+1$ and -1, with instantaneous jumps between them. In contrast, the KP operator can exist at any value in the closed interval $[-1, +1]$, with a continuous transformation between the two states.

Referring to Fig. 3b, we see that the defining elements for a KP operator are

s_1, s_2 = the values of input that determine the width of hysteresis
$r(x)$ = the function that forms the left and the right bounding curves for the hysteresis
a = the rise interval of input over which the operator linearly evolves between the values of -1 and $+1$

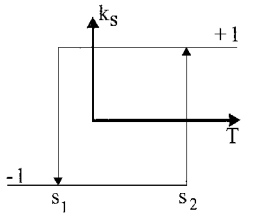

a) Preisach operator

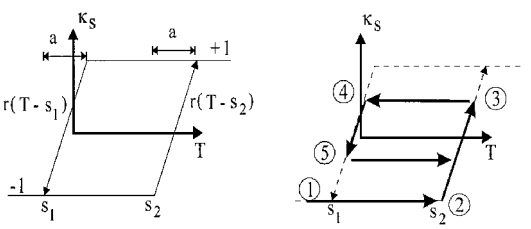

b) KP operator

Fig. 3 Preisach (k_s) and KP (κ_s) operators.

With the above notation, a KP operator is written as κ_s, where $s = (s_1, s_2)$. The function $r(x)$ is given by

$$r(x) = \begin{cases} -1 & x < 0 \\ -1 + 2(x/a) & 0 \le x \le a \\ 1 & x > a \end{cases} \tag{2}$$

The following example illustrates the basic function of the KP operator. Consider the operator shown in Fig. 3b by the dashed line and the input–output relationship for some input history represented by the solid line.

Location 1: v is less than s_1 and $[\kappa_s(v)](t)$ is equal to -1, $\dot{v} > 0$.

Location 2: At this point, $v = s_2$ and $[\kappa_s(v)](t)$ will begin to follow the right bounding curve, $r(v - s_2)$.

Location 3: When $s_2 < v < s_2 + a$, $\dot{v}$ switches sign and v begins to decrease. The output of the operator is recorded with a memory variable, $\xi = [\kappa_s(v)](t)$. As v decreases, $[\kappa_s(v)](t)$ will remain at a value of ξ until $r(v - s_1) < \xi$.

Location 4: When $r(v - s_1) < \xi$, the output will follow the left bounding curve as v decreases.

Location 5: While $v > s_1$, the input switches from decreasing to increasing. The variable ξ is then updated with the new output value, and $[\kappa_s(v)](t)$ will remain at a value of ξ until $r(v - s_2) > \xi$.

The mathematical representation of the KP kernel, as described with the above example, is given by

$$[\kappa_s(v, \xi_s)](t) = \begin{cases} \max[\xi_s, r(v - s_2)] & \text{if} \quad \dot{v} \ge 0 \\ \min[\xi_s, r(v - s_1)] & \text{if} \quad \dot{v} \le 0 \\ (\kappa_s)_{\text{previous}} & \text{if} \quad \dot{v} = 0 \end{cases} \tag{3}$$

where the memory term for a specific operator ξ_s is updated whenever $\dot{v}$ switches sign.

The parameterized KP model is formed from the summation of a finite number of weighted KP operators over a finite region of input, dictated by the interval of input over which hysteresis occurs, say $[v_{\min}, v_{\max}]$. The input interval is discretized into K evenly spaced points. Because there are two values of input defining a KP operator, s_1 and s_2, we require two axes (the s_1 axis and the s_2 axis) to represent decreasing and increasing input, respectively. Close inspection of the operator in Fig. 3b reveals that an operator with switching values $(s_1, s_2) = (v_1, v_2)$ is simply the reverse of an operator with $(s_1, s_2) = (v_2, v_1)$. The conventional approach[8,16] is to choose the set of operators defined by $s_2 \ge s_1$. Hence, in the s_1–s_2 plane, KP operators are defined for $s \in S$, where S is the space of admissable KP operators, defined by

$$S = \{(s_1, s_2): s_1, s_2 \in [v_{\min}, v_{\max}],\ s_2 \ge s_1\} \tag{4}$$

forming the triangle shown in Fig. 4.

For the parameterized KP model, there is a finite number of operators that represent the space S, given by $N = K(K + 1)/2$. Each grid point in Fig. 4 represents a KP operator. If (i, j) indices are created, an individual operator can be denoted by $\kappa_{s_{ij}}$ where

$$s_{ij} = (s_{1i}, s_{2j}), \qquad s_{1i} = v_{\min} + (i - 1)\Delta v$$

$$s_{2j} = v_{\min} + (j - 1)\Delta v, \qquad \Delta v = \frac{v_{\max} - v_{\min}}{K - 1} \tag{5}$$

The one property left to be defined is the rise interval a. From previous numerical studies,[11] a good choice is to set $a = \Delta v$. When the grid-point indices of (i, j) are used, the parameterized KP-hysteresis model can now be defined in the required vector form:

$$[H(v)](t) = \boldsymbol{\theta}^v [\boldsymbol{F}(v)](t)$$

$$\boldsymbol{\theta} = \{\theta_{1,1}, \theta_{1,2}, \ldots, \theta_{1,K}, \theta_{2,2}, \ldots, \theta_{K,K}\}^T$$

$$[\boldsymbol{F}(v)](t) = \left[\left\{\kappa_{s_{1,1}}, \kappa_{s_{1,2}}, \ldots, \kappa_{s_{1,K}}, \kappa_{s_{2,2}}, \ldots, \kappa_{s_{K,K}}\right\}^T\right](t) \tag{6}$$

The development of the inverse KP model is rather involved, and the reader is directed to Refs. 11 and 12 for the full set of equations. We state here that $[H^{-1}(u)](t) = [f(\theta, u, v)](t)$, i.e., the inverse model, is defined by the same set of parameters θ as that of the forward model. Thus any corrections to the forward model to improve the representation of input–output hysteresis will also improve the inverse model.

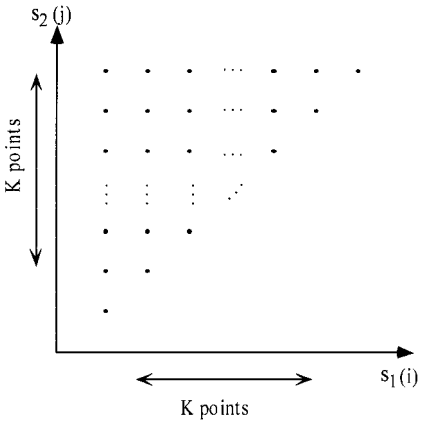

Fig. 4 *S*-plane grid.

III. Model Reference Control with Hysteresis Compensation

This section reviews classical MRC methodology and hysteresis compensation in MRC. Hysteresis compensation involves cases in which the actuator providing the control force to the system plant described in this section exhibits a hysteretic relationship with the input to the actuator. If an exact representation of the hysteresis exists, this nonlinearity can be eliminated, and the desired control from the MRC scheme is what is actually passed to the system plant. However, if the hysteresis can be represented by only an approximate model, then there will be an error injected into the MRC system. Of paramount importance is that this error remain bounded in order for the injected error to enter the system as a bounded disturbance.

A. Model Reference Control

The hysteresis compensation and adaptive-hysteresis update for this paper is used in conjunction with an MRC strategy. This subsection gives a brief discussion of the system and control scheme. A full description of the theory of MRC and model reference adaptive control (MRAC) is presented in Ref. 13. The goal is to drive the plant output y_p to follow a reference model y_m.

The plant model is given by

$$[y_p] = G_p(s)[u_d] \tag{7}$$

where the plant transfer function $G_p(s)$ is given as

$$G_p(s) = k_p \frac{N_p(s)}{D_p(s)} \tag{8}$$

The reference model is given by

$$[y_m] = W_m(s)[r] \tag{9}$$

where

$$W_m(s) = k_m \frac{N_m(s)}{D_m(s)} \tag{10}$$

and $r(t)$ is a reference signal.

The following assumptions (denoted by A1, A2, etc.) are standard for several variants of MRC and MRAC for linear systems (see Ref. 13 or Ref. 19):

A1) The transfer function $G_p(s)$ characterizing the open-loop system has the form of Eq. (8), where $N_p(s)$ and $D_p(s)$ are monic polynomials and $N_p(s)$ is stable and of degree m_p.

A2) An upper bound for the degree n_p of $D_p(s)$ is known.

A3) The relative degree $\eta_p = n_p - m_p$ is known.

A4) The sign of k_p is known.

A5) The transfer function $W_m(s)$ characterizing the reference model has the form of Eq. (10), where $N_m(s)$ and $D_m(s)$ are stable, monic polynomials of degree m_m and n_m, respectively.

A6) The relative degree $\eta_m = n_m - m_m$ of the reference model is equal to the relative degree of the open-loop transfer function $G_p(s)$.

The control u_d for model matching is designed as in

$$u_d = K_1\left(s, \theta_1^*\right)[u] + K_2\left(s, \theta_2^*\right)[y_p] + \theta_3^* y_p + c_0^* r \tag{11}$$

where

$$K_1\left(s, \theta_1^*\right) = \theta_1^{*T}\frac{N_k(s)}{D_k(s)}, \qquad K_2\left(s, \theta_2^*\right) = \theta_2^{*T}\frac{N_k(s)}{D_k(s)}$$

$$c_0^*, \theta_3^* \in R, \qquad \theta_1^*, \theta_2^* \in R^{n-1} \tag{12}$$

$$N_k(s) = \begin{cases} [s^{n-2}, s^{n-3}, \ldots, s, 1]^T & \text{for} \quad n \geq 2 \\ 0 & \text{for} \quad n = 1 \end{cases} \tag{13}$$

$$D_k(s) = \tilde{D}_k(s) N_m(s) \tag{14}$$

If we have a detailed knowledge of the plant $G_p(s)$, conventional MRC techniques introduce the model-matching condition:

$$c_0^* = k_m / k_p \tag{15}$$

$$\theta_1^{*T} N_k(s) D_p(s) + k_p\left[\theta_2^{*T} N_k(s) + \theta_3^* D_k(s)\right] N_p(s)$$

$$= D_k(s) D_p(s) - N_p(s) \tilde{D}_k(s) D_m(s) \tag{16}$$

In an ideal case, Eqs. (15) and (16) are used to calculate the necessary values for $\{\theta_1^*, \theta_2^*, \theta_3^*, c_0^*\}$ such that the closed-loop response obtained by selecting u_d in Eq. (11) renders the response y_p in Eq. (7) to match y_m precisely in Eq. (9).

B. Model Reference Control with Controller Hysteresis Present

When there is a hysteretic relationship between the MRC input u_d to the plant equation (7) and the actual input into the system v, such that $u(t) = [H(v)](t)$, the control strategy is represented by the cascade structure shown in Fig. 5. For this class of problems, it is assumed[14] that 1) the quantity u cannot be explicitly controlled, and 2) u cannot be measured. The actual control input into the system is v, with $u(t) = [H(v)](t)$. A compensator can be designed for the hysteresis nonlinearity with an identified estimate of the hysteresis model $[\hat{H}(v)](t)$ if $\hat{H}^{-1}$ exists.

The plant model given by Eq. (7) then becomes

$$[y_p] = G_p(s)[u] \tag{17}$$

where

$$u(t) = [H(v)](t), \qquad v(t) = [\hat{H}^{-1}(u_d)](t) \tag{18}$$

If the identification of $\hat{H}$ is perfect, i.e., if $\hat{H} = H$ and consequently $\hat{H}^{-1} = H^{-1}$, then

$$u(t) = [H(v)](t) = \left[H\left(\hat{H}^{-1}(u_d)\right)\right](t)$$

$$= \left[H\left(H^{-1}(u_d)\right)\right](t) = u_d(t)$$

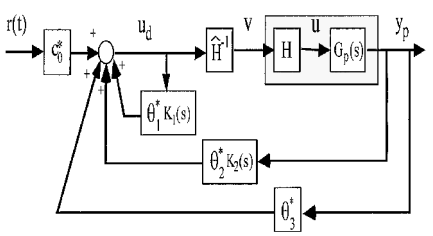

Fig. 5 MRC design with hysteresis present.

and Eq. (17) becomes $y_p = G_p(s)u_d$. However, in practice, $\hat{H}$ cannot be identified exactly, and there is an artificial disturbance injected into the system given by the error between the output of $H(v)$ and its detuned estimate $\hat{H}(v)$. The error e_H between the two models is defined as

$$e_H(t) = u(t) - u_d(t) = [H(v)](t) - [\hat{H}(v)](t) \tag{19}$$

or

$$u(t) = u_d(t) + [H(v)](t) - [\hat{H}(v)](t)$$

$$= u_d(t) + e_H(t)$$

If there exists $\delta^* \geq 0$ such that $|[H(v) - \hat{H}(v)](t)| \leq \delta^*$ for all $v \in V$, then $e_H(t)$ enters into the system as a bounded disturbance.

Theorem 1 (exact hysteresis compensation in MRC):

Consider the plant given by Eq. (17) that has an input nonlinearity $H(v)$ such that $u(t) = [H(v)](t)$ and the reference model given by Eq. (9) such that assumptions A1–A6 hold. Let the fixed linear controller u_d be given by Eq. (11) with constant parameters that satisfy the model-matching equation of Eqs. (15) and (16). Let the exact inverse be such that $\hat{H}^{-1} = H^{-1}$,

$$v(t) = \left[\hat{H}^{-1}(u_d)\right](t) = \left[H^{-1}(u_d)\right](t) \tag{20}$$

initialized by $u(t_0) = H\{H^{-1}[u_d(t_0)]\}$. When Eqs. (11) and (20) are applied to the plant of Eq. (17), all closed-loop signals are bounded and the tracking error $y(t) - y_m(t)$ converges to zero exponentially fast.

Proof: If $\hat{H}^{-1} = H^{-1}$ and $u(t_0) = H\{H^{-1}[u_d(t_0)]\}$, then $u(t) = [H(v)](t) = u_d(t)$ clearly follows from $v(t) = [H^{-1}(u_d)](t)$. The plant model of Eq. (17) then assumes the form of Eq. (7), and all of the properties for MRC without input nonlinearity apply. □

Theorem 1 in simple terms states that if the inverse hysteresis operator is the exact inverse for H, then the inverse $\hat{H}^{-1}$ cancels the effect of H such that u_d can be designed from any linear controller for $G_p(s)$, which ensures the desired system performance. The next theorem establishes a bound on the injected disturbance error and the stability of the resulting closed-loop system when the hysteresis estimate is inexact.

Theorem 2 (inexact hysteresis compensation in MRC):

Consider the plant given by Eq. (17) that has an input nonlinearity $H(v)$ such that $u(t) = [H(v)](t)$ and the reference model given by Eq. (9) such that assumptions A1–A6 hold. Let the fixed linear controller u_d be given by Eq. (11) with constant parameters that satisfy the model-matching condition of Eqs. (15) and (16). Let the exact and the estimated hysteresis models be described by the parameter vectors $\boldsymbol{\theta}$ and $\hat{\theta}$, respectively, satisfying

$$\sum_{k=1}^{K} |\theta_k - \hat{\theta}_k| \leq \delta_\theta$$

Then

1) $u(t) = u_d(t) + e_H(t)$ and $e_H(t) = [H(v)](t) - [\hat{H}(v)](t)$ is a bounded disturbance with the upper bound given by δ_θ, and

$$|e_H(t)| = |[H(v)](t) - [\hat{H}(v)](t)| \leq \delta_\theta$$

for any $(v, \xi_k^0) \in C^0[0, T] \times \mathbb{R}^K$, $v \in V$, $\xi^0 = \hat{\xi}^0$.

2) The closed-loop plant, $y_p = G_p(s)(u_d + e_H)$, is internally stable and there is a constant $\mu^* > 0$ such that for any $\delta_\theta \in [0, \mu^*]$ the tracking error $e = y_p - y_m$ satisfies

$$\lim_{t \to \infty} \sup_{\tau \geq t} |e(\tau)| \leq c\delta_\theta$$

where $c \geq 0$ is a finite constant.

Proof: The proof of part 1 begins by representation of the difference between two KP models, H_{KP} and $\hat{H}_{KP}$, as the summation of

the products of the individual kernel functions and the individual parameter error $\theta_k - \hat{\theta}_k$:

$$
\begin{aligned}
&|H_{\mathrm{KP}}(v) - \hat{H}_{\mathrm{KP}}(v)| \\
&\quad = \left| \sum_{k=1}^{K} \left[k_{s_k}(v, \xi_k)\right](t)\theta_k - \sum_{k=1}^{K} \left[k_{s_k}(v, \xi_k)\right](t)\hat{\theta}_k \right| \\
&\quad = \left| \sum_{k=1}^{K} \left[k_{s_k}(v, \xi_k)\right](t)(\theta_k - \hat{\theta}_k) \right|
\end{aligned}
$$

Simple algebraic manipulation by use of the Schwarz inequality and the fact that the maximum value of an individual kernel function is, by definition, equal to 1, yields the result stated in the theorem:

$$
\begin{aligned}
|H_{\mathrm{KP}}(v) - \hat{H}_{\mathrm{KP}}(v)| &\le \sum_{k=1}^{K} \left| \left[k_{s_k}(v, \xi_k)\right](t) \right| |(\theta_k - \hat{\theta}_k)| \\
&\le \sum_{k=1}^{K} 1|(\theta_k - \hat{\theta}_k)| \\
&\le \delta_\theta
\end{aligned}
$$

Part 2 is simply an application of robust MRC theory with a bounded input disturbance, e.g., theorem 9.3.1 of Ref. 13, pp. 652–653. □

Theorem 2 establishes that when inverse KP model compensation is used in MRC, if the estimated model is not exact, bounds on the resulting input disturbance and resulting model reference error can be quantified in terms of the parameter error. This is ample motivation for developing adaptive laws to update the hysteresis model: As $\hat{\boldsymbol{\theta}}$ approaches $\boldsymbol{\theta}$, the injected disturbance goes to zero and therefore the model reference error goes to zero. In previous work,[11,12] the parameterized KP model was updated by a gradient-adaptive law that did not require any knowledge of the system plant when the hysteresis output can be measured. In the next subsection, we look at the adaptive law for the KP model that incorporates the system plant model dynamics when the hysteresis output cannot be measured.

C. Adaptive-Hysteresis Update Law

From Theorem 2, all MRC signals are bounded when $\hat{H}(v) \neq H(v)$. However, the tracking error, although bounded, will be of a magnitude proportional to $H(v) - \hat{H}(v)$. Therefore we require an adaptive law for updating the hysteresis model parameters $\hat{\Theta}_H(t)$ in order to decrease the tracking error or even drive it to zero. The adaptive law derived in Ref. 14 is stated here. For plant and reference models given by Eqs. (7–10) and the controller equations (11–16), express the tracking error $e(t)$ in terms of the hysteresis model error:

$$
e(t) = [y - y_m](t) = W(s)\tilde{\Theta}_H^T[F(v)](t) \tag{21}
$$

where

$$
\tilde{\Theta}_H = \hat{\Theta}_H - \Theta_H, \qquad W(s) = \frac{1}{c_0^*} W_m(s)\left[1 - \theta_1^* \frac{N_k(s)}{D_k(s)}\right] \tag{22}
$$

Then the adaptive law for $\dot{\hat{\Theta}}_H(t)$ is given by

$$
\dot{\Theta}_H(t) = -\frac{\Gamma \zeta_H(t)\varepsilon_H(t)}{m_H^2(t)} + f_H(t) \tag{23}
$$

where the quantities of Eq. (23) are defined as

$$
\begin{aligned}
\varepsilon_H(t) &= e(t) + \xi_H(t) \\
\xi_H(t) &= \Theta_H^T(t)\zeta_H(t) - W(s)\left[\Theta_H^T F(v)\right](t) \\
\zeta_H(t) &= W(s)[F(v)](t), \qquad m_H^2(t) = 1 + \zeta_H^T(t)\zeta(t) + \xi_H^2(t)
\end{aligned} \tag{24}
$$

and $f_H(t)$ is a projection operator that uses a priori knowledge of the admissible range for $\hat{\Theta}_H$ to ensure signal boundedness. The theorem and the subsequent proof that the adaptive law of Eq. (23) ensures signal boundedness and smallness of the mean characteristics,

$$
\begin{aligned}
\int_{t1}^{t2} \frac{\varepsilon_H^2(t)}{m_H^2(t)}\,\mathrm{d}t &\le a_1 + b_1 \int_{t1}^{t2} \frac{d^2(t)}{m_H^2(t)}\,\mathrm{d}t \\
\int_{t1}^{t2} \|\dot{\Theta}_H(t)\|_2^2\,\mathrm{d}t &\le a_2 + b_2 \int_{t1}^{t2} \frac{d^2(t)}{m_H^2(t)}\,\mathrm{d}t
\end{aligned} \tag{25}
$$

can be found in Ref. 14.

IV. Numerical Examples

In this section, we show the numerical results for MRC with known plant parameters for cases 1) $\hat{H} \neq H$ with fixed compensation and 2) $\hat{H} \neq H$ with adaptive compensation for both constant and time-varying hysteresis plant parameters.

The plant model is given by

$$
y_p = \frac{1}{s^2 + 3s - 10} \tag{26}
$$

The reference model is given by

$$
y_m = \frac{5}{(s+5)^2} \tag{27}
$$

The quantities of the control law of Eq. (11) become

$$
N_k(s) = 1, \qquad D_k(s) = s + 2, \qquad \tilde{D}_k(s) = s + 2 \tag{28}
$$

and the model-matching condition parameters are calculated to be

$$
\begin{Bmatrix} c_0^* \\ \theta_1^* \\ \theta_2^* \\ \theta_3^* \end{Bmatrix} = \begin{Bmatrix} -7 \\ -84 \\ -28 \\ 5 \end{Bmatrix} \tag{29}
$$

The transfer function $W(s)$ is calculated to be

$$
W(s) = k_p\left[\frac{s + \left(2 - \theta_1^*\right)}{s^3 + 12s^2 + 45s + 50}\right] \tag{30}
$$

Define the projection operator f_H to be

$$
f_{H_i} = \begin{cases} 0 & \text{if } \hat{\theta}_{H_i} \in \left(\theta_{H_i}^{\mathrm{lower}}, \theta_{H_i}^{\mathrm{upper}}\right) \\ & \text{or } \hat{\theta}_{H_i} = \theta_{H_i}^{\mathrm{lower}} \text{ and } g_{H_i} \ge 0 \\ & \text{or } \hat{\theta}_{H_i} = \theta_{H_i}^{\mathrm{upper}} \text{ and } g_{H_i} \le 0 \\ -g_{H_i} & \text{otherwise} \end{cases} \tag{31}
$$

where g_{H_i} is the first expression of Eq. (23).

In the first set of experiments, the hysteresis plant is represented by a constant set of parameters, θ^*, with the specific values listed in Table 1. The estimated hysteresis model is represented in Table 1, which serves as the initial guess for the adaptive model. Figure 6a shows the reference model y_m trajectory for $r(t) = 10\sin(1.1t)$. The corresponding tracking errors $e(t) = y(t) - y_m(t)$ and hysteresis model errors $e_H(t) = u(t) - u_d(t)$ for using fixed (dashed curves) and adaptive (solid curves) compensation are shown in Figs. 6b and 6c, respectively. With the fixed-hysteresis model, the actuator error is bounded, but does not decrease in magnitude. This results in a bounded tracking error that also remains at a fixed amplitude. However, one can see that the adaptive-hysteresis model learns the actuator hysteresis over time, and $e(t) \to 0$ as $e_H(t) \to 0$.

For the reference signal $r(t) = 10\sin(1.1t)$, the resulting input-output hysteresis occurs between the same two dominant input extrema and forms a single hysteresis loop. A second numerical experiment was conducted for a reference signal given by the sum of two

Table 1 Hysteresis plant (representing actuator hysteresis) and hysteresis model estimate

Characteristic	Hysteresis plant (actuator)	Estimated model (initial guess)
Discretization number	$K = 20$ $(N = 210$ parameters$)$	$K = 13$ $(N = 91$ parameters$)$
Hysteresis region	$s_{\min} = 10, s_{\max} = 60, \quad v \in [10, 60 + a]$	$s_{\min} = 0, s_{\max} = 70, \quad v \in [0, 70 + a]$
Rise constant	$a = \Delta s = \dfrac{60 - 10}{19} = 2.63$	$a = \Delta s = \dfrac{70 - 0}{12} = 5.83$
Parameters	$\bar{\theta}_{ij} = \exp\left[\dfrac{-(s_i - 35)^2(s_j - 35)^2}{4 \times 10^4}\right]$	$\bar{\theta}_{ij} = \exp\left[\dfrac{-(s_i - 35)^2(s_j - 35)^2}{4 \times 10^4}\right]$
	$s_i = s_{\min} + (i - 1)\Delta s$	$s_i = s_{\min} + (i - 1)\Delta s$
	$s_j = s_{\min} + (j - 1)\Delta s$	$s_j = s_{\min} + (j - 1)\Delta s$
	$\theta^*_{ij} = \dfrac{40\,\bar{\theta}_{ij}}{\sum_{i,j} \bar{\theta}_{ij}}$	$\hat{\theta}_{ij} = \dfrac{40\,\bar{\theta}_{ij}}{\sum_{i,j} \bar{\theta}_{ij}}$

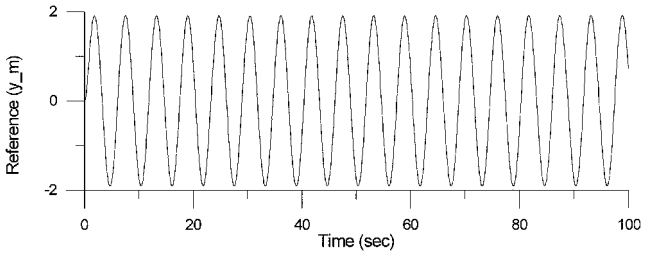

a) Reference model output, $y_m(t)$

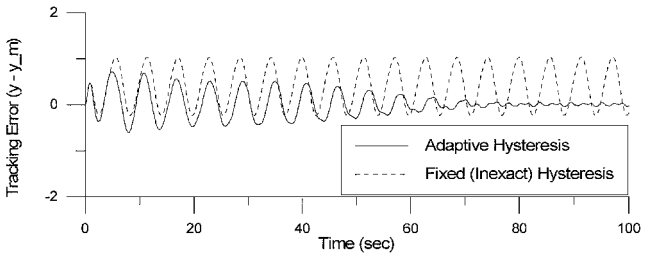

b) System tracking error, $e(t) = y(t) - y_m(t)$

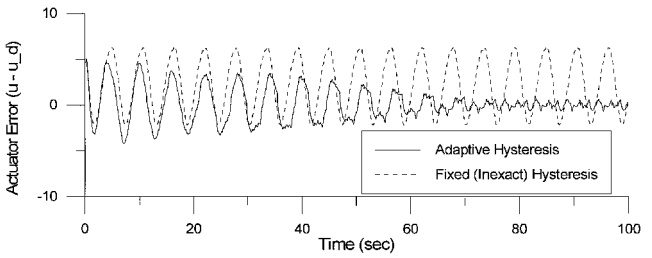

c) Injected hysteresis error, $e_H(t) = u(t) - [\hat{H}(v)](t)$

Fig. 6 MRC tracking experiment with fixed-hysteresis (inexact) and adaptive-hysteresis compensation for reference signal $r(t) = 10 \sin(1.1t)$.

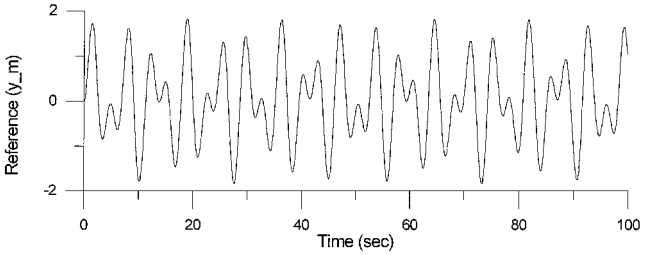

a) Reference model output, $y_m(t)$

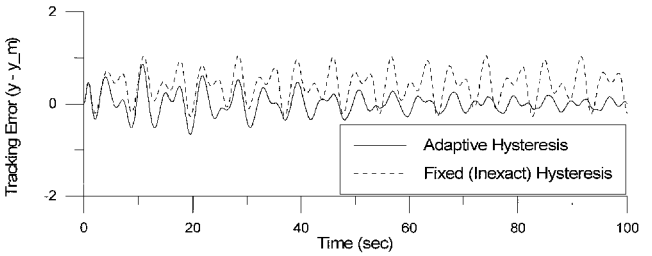

b) System tracking error, $e(t) = y(t) - y_m(t)$

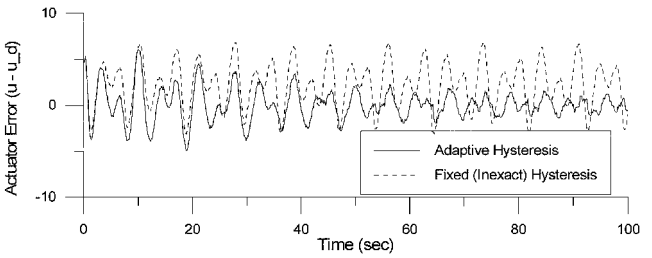

c) Injected hysteresis error, $e_H(t) = u(t) - [\hat{H}(v)](t)$

Fig. 7 MRC tracking experiment with fixed-hysteresis (inexact) and adaptive-hysteresis compensation for reference signal $r(t) = 10\{0.5 \sin(1.1t) + 0.5 \sin[\sqrt{(3.2)}t]\}$.

sinusoids as $r(t) = 10\{0.5 \sin(1.1t) + 0.5 \sin[\sqrt{(3.2)}t]\}$ with non-periodic frequencies. This constitutes a more difficult case because the actuator will encounter varying dominant input extrema, resulting in multiple inner loops, i.e., more hysteresis nonlinearities will be exhibited. The results for this second experiment are displayed in Fig. 7. Clearly, the reference trajectory y_m is more complicated than that shown in Fig. 6. The results for fixed and adaptive compensation have the same trend as in the experiment of Fig. 6; however, in this case more time is required for the adaptive hysteresis model to learn the actuator hysteresis.

In the above two numerical experiments, the model representing the actuator hysteresis was designed with constant parameters and the estimated hysteresis model was initially not equal to the exact hysteresis. The next experiment examines the performance of the fixed- and the adaptive-hysteresis models in MRC when the plant hysteresis is evolving, i.e., time-varying plant parameters. In this case, the two models begin equal to the $K = 13$ model listed in Table 1. The plant parameters are designed to evolve over time such that $\theta^*_{ij}(t) = \theta^*_{ij}(0)(1 + t/200)$. Figure 8a shows the evolution of the major-loop plant hysteresis from $t = 0$ to 200. For a reference signal given by $r(t) = 10 \sin(1.1t)$, the tracking error and the actuator output error for both fixed (dashed curves) and adaptive (solid curves) compensation are shown in Figs. 8b and 8c. Initially, $e(t)$ and $e_H(t)$ are zero because $\hat{H} = H^*$. However, as $\theta^*(t)$ evolves, the actuator error (for fixed compensation) grows, injecting increasingly larger input disturbances into the MRC controller, and the system tracking error becomes larger. With adaptive compensation, Fig. 8 shows that the growth of $e_H(t)$ is stabilized because the estimated model is evolving to match the variation in the hysteresis plant.

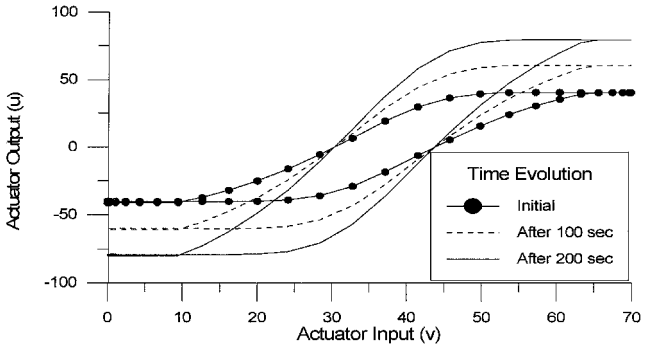

a) Time-evolution of hysteresis plant

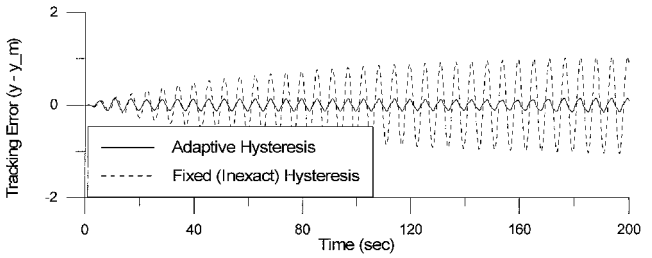

b) System tracking error, $e(t) = y(t) - y_m(t)$

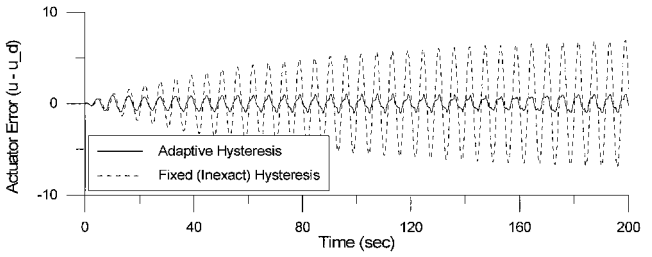

c) Injected hysteresis error, $e_H(t) = u(t) - [\hat{H}(v)](t)$

Fig. 8 Time-varying hysteresis plant, MRC tracking experiment with fixed-hysteresis (inexact) and adaptive-hysteresis compensation for reference signal $r(t) = 5 \sin(2.6t)$.

V. Conclusions

In both numerical experiments with a generic hysteresis actuator representation and laboratory experiments with SMA actuators, previous works[11,12] by the authors have shown excellent performance of the gradient-adaptive KP-hysteresis model. The gradient-adaptive law requires at least an estimate of the actuator output measurement. When the actuator output is a quantity linked to actuator displacement (such as strain vs temperature, for SMA), these measurements are relatively simple to acquire experimentally. However, the parameterized KP model is not limited to describing this type of hysteresis, but can be used to describe quantities that cannot be directly measured, such as force, viscosity, and magnetism. Therefore this paper extends the model to adaptive control strategies in which the hysteresis output measurements are assumed to be unknown and the adaptive update relies solely on system output measurements.

Theorems necessary for the incorporation of the parameterized KP model as an inverse model compensator in MRC were provided. Numerical examples showed the effectiveness of using the adaptive model compared with a fixed model. In addition, it was shown that the adaptive model also works well when the actuator hysteresis properties are time varying.

Acknowledgments

The authors acknowledge the financial support of the U.S. Army Research Office, Contract DAAL 03-92-G-0123, monitored by G. L. Anderson for the early part of this work. Partial support by the U.S. Office of Naval Research, Grant N00014-97-1-0943 (Allen Moshfegh, program monitor), and the Texas Higher Education Coordinating Board, Grant ATP-03627-081, is also acknowledged.

References

[1]Hughes, D., and Wen, J., "Preisach Modeling of Piezoceramic Hysteresis: Independent Stress Effect," *Smart Structures and Materials 1995: Mathematics and Control in Smart Structures*, edited by V. V. Varadan, Proceedings of the SPIE, Vol. 2442, pp. 328–336; Springer–Verlag, Berlin, May 1995.

[2]Ge, P., and Jouaneh, M., "Tracking and Control of a Piezoceramic Actuator," *IEEE Transactions on Control Systems Technology*, Vol. 4, 1996, pp. 209–215.

[3]Liang, C., and Rogers, C., "One-Dimensional Thermomechanical Constitutive Relations of Shape Memory Materials," *Journal of Intelligent Material Systems and Structures*, Vol. 1, April 1990, pp. 1–20.

[4]Lagoudas, D., Bo, Z., and Qidwai, M., "A Unified Thermodynamic Constitutive Model for SMA and Finite Element Analysis of Active Metal Matrix Composites," *Mechanics of Composite Structures*, Vol. 3, 1996, pp. 153–179.

[5]Kamath, G., and Wereley, N. M., "Nonlinear Viscoelastic-Plastic Mechanisms-Based Model of an Electrorheological Damper," *Journal of Guidance, Control, and Dynamics*, Vol. 20, 1997, pp. 1125–1132.

[6]Krasnosel'skii, M., and Pokrovskii, A., *Systems with Hysteresis*, Springer–Verlag, Berlin, 1989.

[7]Visintin, A., *Differential Models of Hysteresis*, Springer–Verlag, Berlin, 1994.

[8]Mayergoyz, I., *Mathematical Models of Hysteresis*, Springer–Verlag, Berlin, 1991.

[9]Verdi, C., and Visintin, A., "Numerical Approximation of Hysteresis Problems," *IMA Journal of Numerical Analysis*, Vol. 5, 1985, pp. 447–463.

[10]Verdi, C., and Visintin, A., "Numerical Approximation of the Preisach Model for Hysteresis," *Mathematical Modelling and Numerical Analysis*, Vol. 23, 1989, pp. 335–356.

[11]Webb, G., "Adaptive Identification and Compensation for a Class of Hysteresis Operators," Ph.D. Dissertation, Dept. of Aerospace Engineering, Texas A&M University, College Station, TX, May 1998.

[12]Webb, G. V., Kurdila, A. J., and Lagoudas, D. C., "Hysteresis Modeling of SMA Actuators for Control Applications," *Journal of Intelligent Material Systems and Structures*, Vol. 9, No. 6, 1998, pp. 432–448.

[13]Ioannou, P., and Sun, J., *Robust Adaptive Control*, Prentice–Hall, Englewood Cliffs, NJ, 1996.

[14]Tao, G., and Kokotovic, P., *Adaptive Control of Systems with Actuator and Sensor Nonlinearities*, Wiley, New York, 1996.

[15]Tao, G., and Kokotovic, P., "Adaptive Control of Plants with Unknown Hysteresis," *IEEE Transactions on Automatic Control*, Vol. 40, Feb. 1995, pp. 200–212.

[16]Banks, H., Kurdila, A., and Webb, G., "Modeling and Identification of Hysteresis in Active Material Actuators, Part (II): Convergent Approximations," *Journal of Intelligent Material Systems and Structures*, Vol. 8, No. 6, 1997.

[17]Preisach, F., "Uber die Magnetische Nachwirkung," *Zeitschrift für Physik*, Vol. 94, 1935, pp. 277–302.

[18]Banks, H., Kurdila, A., and Webb, G., "Identification of Hysteretic Control Influence Operators Representing Smart Actuators: Formulation," TR CRSC-TR96-14, Center for Research in Scientific Computation, North Carolina State Univ., Raleigh, NC, 1996.

[19]Sastry, S., and Bodson, M., *Adaptive Control*, Prentice–Hall, Englewood Cliffs, NJ, 1989.